Involvement of ERK1/2 activation in the gene expression of senescence-associated secretory factors in human hepatic stellate cells

Involvement of ERK1/2 activation in the gene expression of senescence-associated secretory factors in human hepatic stellate cells

Naoshi Odagiri, Tsutomu Matsubara, Moe Higuchi, Sayuri Takada, Hayato Urushima, Misako Sato-Matsubara, Yuga Teranishi, Katsutoshi Yoshizato, Norifumi Kawada, Kazuo Ikeda

Title：Involvement of ERK1/2 activation in the gene expression of senescence-associated secretory factors in human hepatic stellate cells.

Naoshi Odagiri[1,2], Tsutomu Matsubara[1,*], Moe Higuchi[1], Sayuri Takada[1,2], Hayato Urushima[1], Misako Sato-Matsubara[2,3], Yuga Teranishi[2], Katsutoshi Yoshizato[3,4], Norifumi Kawada[2], Kazuo Ikeda[1].

1. Department of Anatomy and Regenerative Biology, Osaka City University Graduate School of Medicine, Osaka, 545-8585, Japan
2. Department of Hepatology, Osaka City University Graduate School of Medicine, Osaka, 545-8585, Japan.
3. Endowed Laboratory of Synthetic Biology, Osaka City University Graduate School of Medicine, Osaka, 545-8585, Japan
4. Academic advisor's office of PhoenixBio Co. Ltd, Higashihiroshima, 739-0046, Japan

[*]**Correspondence:** Tsutomu Matsubara, Department of Anatomy and Regenerative Biology, Osaka City University Graduate School of Medicine, Osaka, 545-8585, Japan, Tel: +81-6-6645-3701, Fax: +81-6-6645-3702, Email: matsu335@med.osaka-cu.ac.jp

Abstract

Senescent hepatic stellate cells (senescent HSCs) are found in patients with liver cirrhosis and have been thought to be involved in the development of hepatocellular carcinoma (HCC) in mice via the senescence-associated secretory proteins. However, in humans, which secretory proteins are involved and what regulate their expression remain unclear. In the current study, we characterized senescence-associated β-galactosidase-positive senescent human HSCs (hHSCs) induced by repetitive passaging. They exhibited enhanced expression of 14 genes for secretory protein and persistent phosphorylation of ERK1/2 protein but not JNK or p38 MAPK proteins. Enhanced nuclear ERK1/2 phosphorylation was observed in senescent hHSCs. Treatment of the senescent hHSCs with ERK1/2 inhibitor, SCH772984, significantly decreased the levels of angiopoietin like 4 (ANGPTL4), C-C motif chemokine ligand 7 (CCL7), Interleukin-8 (IL-8), platelet factor 4 variant 1 (PF4V1), and TNF superfamily member 15 (TNFSF15) mRNA levels in a dose-dependent manner. The enhanced phosphorylation of ERK1/2 and expression of *ANGPTL4*, *IL-8* and *PF4V1* genes were observed in both of senescent human dermal fibroblasts and X-ray-induced senescent hHSCs. However, transient ERK1/2 activation induced by epidermal growth factor could not mimic the gene profile of the senescent hHSCs. These results revealed involvement of ERK1/2 signalling in the regulation of senescence-associated secretory factors, suggesting that simultaneous induction of *ANGPTL4*, *IL-8*, and *PF4V1* genes is a marker

of hHSC senescence. This study will contribute to understanding roles of senescent hHSCs in liver diseases.

Keywords

Hepatic stellate cell; Senescence; Secretory factor; ERK1/2; Fibroblast

Introduction

Cellular senescence is recognized as an irreversible cell cycle arrest and is induced by replicative exhaustion [1] or various stresses with cellular damage [2,3]. The senescence of epithelial cells has been generally thought to restrict tumour progression [4]. On the other hand, the senescence of stromal cells, such as fibroblasts, has been reported to show a pro-tumourigenic effect in the breast [5-7], oral cavity [8], and prostate [9], altering the secretory protein profile (also called senescence-associated secretory phenotype). The senescence-associated secretory proteins are various bioactive factors composed mainly of soluble signaling factors (e.g. interleukins, chemokines, and growth factors), secreted proteases, or extracellular matrix (ECM) components and are believed to be major factors for the cancer progression.

Liver cirrhosis is late-stage chronic hepatitis that is independent of the pathogenesis of hepatitis, following alteration of the microenvironment with chronic inflammation. Alteration of the microenvironment involves hepatic stellate cells (HSCs), the main stromal cell type in the liver. HSCs become a myofibroblast-like form following various liver injuries (the formation is called activation) and activated HSCs show accelerated production of secretory proteins such as ECM components, cytokines, and chemokines. Continuous HSC activation alters the hepatic microenvironments with excessive ECM accumulation, resulting in cirrhosis and liver failure [10]. In addition, senescent HSCs have also been observed in patients with liver cirrhosis, probably

derived from activated HSCs [11]. Since their discovery, senescent HSCs have been studied and reported to be involved in the pathophysiology of chronic liver disorders such as cirrhosis or hepatocellular carcinoma (HCC) using mouse models. However, the function of senescent HSCs in HCC is not fully understood. Lujambio *et al.* reported that p53-positive senescent HSCs release factors that skew macrophage polarization towards a tumour-inhibiting M1-state capable of attacking senescent cells in culture [12]. In contrast, Yoshimoto *et al.* demonstrated that alterations in gut microbiota induced by obesity increased the levels of deoxycholic acid provoking the senescence-associated secretory phenotype in HSCs through enterohepatic circulation, resulting in HCC [13]. In particular, in humans, characterization of senescent HSCs remains insufficient.

In the present study, we searched the gene expression profiles of senescent hHSCs for senescence-associated secretory genes and investigated the gene regulation following cell senescence to understand the characteristics of senescent HSCs. Thus, we identified three senescence-associated secretory genes whose expression levels were up-regulated by ERK1/2 signalling in senescent hHSCs.

Materials and methods

Materials

Human recombinant epidermal growth factor (EGF) was obtained from PROSPEC (East Brunswick, NJ, USA). SCH772984 (ERK inhibitor) was purchased from Cayman Chemical (Ann Arbor, MI, USA). Primary antibodies were purchased from Cell Signaling Technology (Danvers, MA, USA), Abcam (Cambridge, UK), Santa Cruz Biotechnology (Dallas, TX, USA), and Millipore (Billerica, MA, USA) as shown in Table 1. Secondary antibodies for western blot analysis, anti-rabbit IgG (Cat. #7074) and anti-mouse IgG (Cat. #7076), were purchased from Cell Signaling Technology. The other chemicals were obtained from FUJIFILM Wako Pure Chemical Corporation (Osaka, Japan) unless otherwise specified.

Cell culture and senescence induction

The human hepatic stellate cell line HHSteCs (Lot #4630 and #10326 designated as "Lot 1" and "Lot 2", respectively), derived from two individuals, were purchased from ScienCell Research Laboratories (Carlsbad, CA, USA). These cells were maintained using the Stellate Cell Medium set (Cat. #5301) at 37 °C in a humidified 5% CO_2 atmosphere. Senescent HHSteCs were generated by repetitive passaging or 20 Gy of X-ray irradiation. Human dermal fibroblasts (hDFs) were obtained as previously reported [14] and were maintained with DMEM at 37 °C in a 5%

CO_2 atmosphere. Senescent hDFs were generated by repetitive passaging.

Doubling-time calculation and senescence-associated β-galactosidase (SA-βGal) staining

The doubling time (DT) was evaluated by cell counting using the Cell Counter Plate (Watson, Tokyo, Japan) for each cell passage. The number of cells, which were seeded initially, was 5×10^5 cells/dish. DT was calculated using the following formula; $DT = T/\log_2 (P/P_0)$ [T is interval time from previous passage (days); P is the number of cells at cell passage; P_0 is the number of cells seeded initially]. SA-βGal positive cells were identified using the Cellular Senescence Detection Kit (CELL BIOLABS, San Diego, CA, USA) according to the manufacturer's instructions.

RNA analysis and microarray analysis

RNA was extracted from cells using TRIzol reagent (Thermo Fisher Scientific, Waltham, MA, USA) and Direct-zol RNA Miniprep (Zymo Research, Irvine, CA, USA). A gene expression array was performed using the SurePrint G3 Human GE 8×60K v2 Microarray by Takara Bio Inc. (Shiga, Japan). Quantitative PCR (qPCR) was performed using cDNA generated from RNA and the SuperScript III Reverse Transcriptase kit (Thermo Fisher Scientific). The primers used in this study are listed in Table 2. The qPCR reaction was carried out using the SYBR green PCR master mix (Thermo Fisher Scientific) in the Thermal Cycler Dice Real Time System 2 (TAKARA BIO,

Shiga, Japan). The values were quantified using the comparative CT method and were normalized to 18S ribosomal RNA. The data were expressed as the ratio to the average of the normal cell group (NC) or control group.

Histone extraction

For western blot analysis of H2A histone family member X (H2AX) and phosphorylated H2AX (γH2AX), the protein samples were pretreated with hydrochloric acid to extract histone from cells according to the histone extraction protocol provided by Abcam. Briefly, HHSteCs were washed with ice-cold phosphate-buffered saline (PBS) and were suspended in the Triton extraction buffer (TEB: PBS containing 0.5% (v/v) Triton X 100, 2 mM phenylmethylsulphonyl fluoride, 0.02% (w/v) NaN_3). After incubation on ice for 10 min, the suspension was centrifuged (2000 rpm, 4 °C, 10 min). After the supernatant was discarded, the cell pellet was washed with TEB. The cell pellet was suspended with 0.2 M HCl and incubated at 4 °C overnight. After centrifugation (2000 rpm, 4 °C, 10 min), the supernatant was subjected to western blot analysis.

Western blot analysis

Cells were homogenized with RIPA buffer (50 mM Tris-HCl at pH 7.5, 150 mM NaCl, 1% Triton X-100, 1% SDS) containing the protease inhibitor cocktail cOmplete Mini (Roche, Basel,

Switzerland) and phosphatase inhibitors (1 mM sodium fluoride, 1 mM β-glycerol phosphate, and 1 mM sodium vanadate). Protein samples were subjected to 8-15% SDS-polyacrylamide gel electrophoresis and were transferred to polyvinylidene difluoride membranes using standard western blotting techniques. After blocking with 5% skim milk, the membranes were probed with primary antibodies diluted at 1:1000 and horseradish peroxidase-conjugated secondary antibodies diluted at 1:5000. Immunoreactive bands were visualized using the ImmunoStar Zeta or ImmunoStar LD system and were detected using the LAS3000 or LAS4000 device (GE healthcare, Chicago, IL, USA). WB Stripping Solution (Nacalai tesque, Kyoto, Japan) was used to remove the antibodies from the western blot membrane.

Flow cytometry analysis

The amount of DNA per haploid was analysed using Vybrant DyeCycle Green (Thermo Fisher Scientific). Diploid and tetraploid fractions were detected using the LSR II Flow Cytometer (BD Biosciences, NJ, USA) after incubation with Vybrant DyeCycle Green.

Immunohistochemistry

HHSteCs or hDFs were seeded on chamber slides (Matsunami Glass Industry Ltd, Osaka, Japan). After washed with PBS containing 0.1% Tween® 20 (PBS-T), The cells were fixed with 4%

paraformaldehyde phosphate buffer solution (Nakalai tesque) for 1 hr at room temperature. Next, the fixed cells were pre-incubated with 3% bovine serum albumin (BSA)/PBS-T for 1 hr at room temperature after the cells were washed with PBS-T, and subsequently incubated with primary antibody against DNA replication factor Cdt1 (CDT1) (Abcam, 1:100 dilution) or $p21^{Waf1/Cip1}$ (Cell Signaling Technology, 1:100 dilution) at 4 °C. After overnight incubation, the cells were washed with PBS-T and incubated with secondary antibody AlexaFluor 594 goat anti-mouse IgG (Molecular Probes, Eugene, OR, USA) for 30 min at room temperature. After adding DAPI (4',6-diamidino-2-phenylindole), the cells were washed and mounted with ProLong Gold Antifade Reagent (Molecular Probes, Eugene, OR, USA). The resulting cells were evaluated by BZ-X710 microscopy (Keyence, Osaka, Japan).

Enzyme-linked immunosorbent assay (ELISA)

Culture medium were collected after incubation with cells for 2 days. IL-8 concentration in the medium was determined using the Human IL-8 ELISA MAX™ Standard Sets (BioLegend, San Diego, CA).

Isolation of nuclear proteins from cells

Normal and senescent cells were washed twice with cold-PBS and then these nuclear and

cytosolic proteins of the cells were fractionated with Qproteome Cell Compartment Kit (QIAGEN, Nordrhein-Westfalen, Germany). Cytosol fraction of SCs was used to check a contamination of cytosolic protein in nuclear fraction.

EGF stimulation

HHSteCs were seeded and cultured in SteCM media for 1 day. The medium was changed to DMEM without foetal bovine serum for starvation (7 hr), and then EGF (diluted with 0.1% BSA) was directly added to the DMEM. The BSA solution, used for the vehicle, was added to the untreated group. The cells were collected after incubation for 15 min (for western blot analysis) and 48 hr (for qPCR and western blot analysis).

Statistical analysis

Statistical analysis was performed using Prism version 6.0 software (GraphPad Software, San Diego, CA, USA). A p-value of less than 0.05 was considered as a significant difference.

Results

Generation of senescent human HSCs using repetitive passaging.

HHSteCs were cultured to establish a senescent model of human HSCs. The more HHSteCs were passaged, the more the doubling time increased (Fig.1A). When the passage number was more than twenty, the cells showed strong senescence-associated β-galactosidase (SA-βGal) staining without enhanced mRNA levels of galactosidase beta 1 (GLB1) believed to be the origin of SA-βGal [15], and the percentage ratio of the SA-βGal-positive cell number to the total cell number was more than 70% (Fig. 1B), while that in the control cells was less than 20%. Thus, more than 70% of cells represented senescent cells (SCs) and less than 20% represented normal cells (NCs), respectively. In addition, SCs enhanced phosphorylated H2A histone family member X protein (γH2AX), a known DNA damage marker, and increased the protein expression level of $p21^{Waf1/Cip1}$ protein (Fig.1C), which was used as a senescence marker of HSCs in human fibrotic livers [11]. Furthermore, SC increased the number of tetraploid cells without changing the number of CDT1 (a specific protein for G1 phase in the cell cycle)-positive cells (Figs. 1D and 1E). Thus, considering a previous report that tetraploid cells with CDT1 expression are senescent cells [16], the latter was generated from HHSteCs. Using the senescent cells, we investigated the mRNA levels of HSC-related genes [alpha-smooth muscle actin (αSMA), collagen type I alpha 1 (COL1A1), collagen type I alpha 2 (COL1A2), peroxisome proliferator-activated receptor gamma

(PPARγ), and cytoglobin (CYGB)]. Unlike the gene profile of activated HSCs, the expression levels of αSMA, COL1A1, COL1A2 and CYGB mRNAs were not changed in SCs, although the PPARγ mRNA levels were decreased (Fig.1F). Next, the level of interleukin (IL)-8, IL-1β, IL-6, vascular endothelial growth factor (VEGF) and serpin family E member 1 (SERPINE1), reported previously as senescence-associated secretory factors, were measured. Only IL-8 mRNA levels were increased in the SC (Fig.1F). Additionally enzyme-linked immunosorbent assay (ELISA) indicated significantly high IL-8 concentration in the culture medium of the SCs, compared to that of the NCs (Fig.1G).

Investigation of senescence-associated secretory factors in human HSCs

Microarray analysis was performed to capture senescence-associated secretory factors more broadly and investigate a gene regulation of senescence-associated secretory factors in the senescent HSCs. When cut-off value was 2-fold, more than 100 genes were indicated as up-regulated senescence-associated secretory gene and the number was too many to perform the quantitative PCR, In this study, we decided to use 4.5-fold as the cut-off value including the SAA genes which were upregulated in human mesenchymal stem cells during in vitro aging [17]. From the obtained results, twenty five of the highly upregulated genes in SCs were related to secretory protein (Fig. 2A and Table 3). Among the 25 genes, the elevated expression of 14 genes (ANGPT1,

ANGPTL4, BMP4, CCL2, CCL7, IL-8, CYTL1, IGFBP3, PF4V1, RARRES2, SAA1, SAA2, TNFRSF11B, and TNFSF15) was indicated by qPCR (Figs. 2B and 2C). Thus, we determined whether the 14 genes could serve as senescence-associated secretory factors in hHSCs.

Involvement of ERK1/2 in the expression of senescence-associated secretory factors in hHSCs.

The phosphorylation levels of major mitogen-activated protein kinases were measured to understand which pathways were activated in senescent HSCs. The phosphorylation levels of ERK1/2, but not those of JNK nor p38, were significantly increased in SCs (Figs.3A and 3B), although MEK1/2 phosphorylation was not changed (Fig.3B). Interestingly, enhanced ERK1/2 phosphorylation was observed in nuclear fraction of the SCs (Fig.3C). Additionally, lamin B1 (LMNB1) was decreased in nucleus of SCs as previously reported [18,19]. In addition, treatment with the ERK1/2-inhibitor SCH772984 significantly decreased the mRNA levels of ANGPTL4, CCL7, IL-8, PF4V1, and TNFSF15 in a dose-dependent manner (0.2-, 0.3-, 0.2-, 0.6-, and 0.2-fold at 100 nM, respectively), as shown in Fig.3D. Enhanced ERK1/2 phosphorylation was observed when the doubling time was increased (Figs. 1A and 3E). To investigate whether transient ERK1/2 activation induced the expression of senescence-associated secretory factors, we tested normal HHSteCs with epithelial growth factor (EGF), an activator of the ERK1/2

signalling. Transient ERK1/2 activation could not mimic the gene profile of SCs (Figs. 3F and 3G). Taken together, these results indicated that consecutive ERK1/2 activation leads to the induction of senescence-associated secretory factor expression.

Expression levels of the ERK1/2-related genes are increased in senescent human dermal fibroblasts.

To investigate whether the induction of *ANGPTL4*, *CCL7*, *IL-8*, *PF4V1* and *TNFSF15* gene expression with ERK1/2 activation is specific in senescent HSCs, we generated senescent human dermal fibroblasts (hDFs) by repetitive passages. Senescent hDFs exhibited obviously increased SA-βGal activity, independent of *GLB1* gene expression (Fig.4A). Interestingly, senescent hDFs also enhanced ERK1/2 phosphorylation (Fig.4B) and $p21^{Waf1/Cip1}$ expression (Figs.4B and 4C) and elevated the mRNA levels of ANGPTL4, CCL7, IL-8, PF4V1, and TNFSF15 (Fig.4D). In addition, increased concentration of IL-8 protein was clearly observed in culture medium of senescent hDFs (Fig.4E). Taken together, the data strongly support a possibility that ERK1/2 activation is a common process of cell senescence in fibroblastic cells.

Enhanced ERK1/2 phosphorylation and induction of *ANGPTL4*, *IL-8* and *PF4V1* gene expressions were also observed in the X-ray-induced senescent HSCs.

Using another model X-ray-induced cell senescence, we investigated whether ERK1/2 activation was enhanced and whether the mRNA levels of ANGPTL4, CCL7, IL-8, PF4V1, and TNFSF15 were increased in senescent HSCs. The X-ray-induced senescent HSCs exhibited obviously increased SA-βGal staining (Fig.5A). Increased $p21^{Waf1/Cip1}$ protein levels and enhanced phosphorylation of ERK1/2 were observed in X-ray-induced senescent HSCs (Fig.5B), as well as in passage-induced senescent HSCs. Enhanced ERK1/2 phosphorylation appeared 24 hr after exposure to X-ray irradiation, following induction of $p21^{Waf1/Cip1}$ expression (Fig.5C). The mRNA levels of ANGPTL4, IL-8 and PF4V1 were significantly increased in both of senescent Lot1 and Lot2 cells, while those of CCL7 and TNFSF15 mRNA were increased in Lot2 cells but not in Lot1 cells (Fig.5D). These senescent cells showed elevated concentration of IL-8 protein in the culture medium as well as the passage-induced senescent cells (Fig.5E). These results may indicate that the simultaneous event of *ANGPTL4*, *IL-8*, and *PF4V1* gene induction by ERK1/2 activation is a common phenomenon in senescent hHSCs.

Discussion

The current study investigated the gene expression profile of senescent human HSCs *in vitro,* utilizing senescent HSC models derived from HHSteCs, and demonstrated that ERK1/2 phosphorylation was enhanced in senescent hHSCs and was involved in the expressions of *ANGPTL4*, *IL-8* and *PF4V1* genes. Interestingly, enhanced ERK1/2 phosphorylation and induced *ANGPTL4*, *IL-8* and *PF4V1* expressions were not only observed in passage-induced senescent hHSCs but also in X ray-induced senescent hHSCs and senescent hDFs.

Our results suggest that ERK1/2 activation is a common senescence-associated factor in fibroblastic cells and is involved in the gene regulation of senescence-associated secretory factors (ANGPTL4, IL-8 and PF4V1). Phosphorylated ERK1/2 was increased in nucleus of senescent HSCs, which strongly supports that ERK1/2 activation plays a role of senescence-associated gene regulation in the HSCs. However, transient ERK1/2 activation (EGF treatment) could not fully mimic the gene expression profile of senescent HSCs in normal HSCs. These results may indicate a requirement of continuous ERK1/2 activation or involvement of other senescence-associated factors in gene regulation. Reduced activities of protein phosphatases 1 and 2A was reported to be involved in senescence-associated activation of ERK1/2 in normal human diploid fibroblasts [20]. Decreased activities of the phosphatases may be important to elevate ERK1/2 phosphorylation in the senescent HSCs. Senescence-associated secretory factors have been demonstrated to be regulated by NF-κB [21], CCAAT/enhancer-binding protein beta [22], p38

[23], and mammalian target of rapamycin signaling [24,25]. Further study of the interaction between ERK1/2 and these factors is also needed to fully understand the related regulatory mechanisms.

ANGPTL4, IL-8, and PF4V1 have been reported to be associated with the progression of various cancers. For example, ANGPTL4 is a factor involved in the progression of human colorectal cancer, especially venous invasion and distant metastasis [26]. Increased expression of IL-8 in the tumour microenvironment enhanced the growth and metastasis of colon cancer [27]. In addition, endogenous PF4V1 (also known as CXCL4L1) promoted the growth of pancreatic ductal adenocarcinoma (Panc-1 cells), independently of its anti-angiogenic function [28]. Furthermore, IL-8 and ANGPTL4 are also known to accelerate the progression of HCC; Zhu *et al*. demonstrated that activated HSCs within the stroma of HCC contributed to tumour angiogenesis via IL-8 [29]; Li *et al*. suggested that ANGPTL4 could significantly promote HCC cell invasion and metastasis *in vitro* and *in vivo* [30]. Taken together, these observations and the current study suggest that senescent HSCs affect the microenvironment surrounding HCC through the secretion of ANGPTL4, IL-8 and PF4V1. In this study, the induction of these genes was regulated by ERK1/2 in the senescent HSCs. Sorafenib, a multiple receptor tyrosine kinase inhibitor that also targets ERK1/2, is a recommended drug for advanced HCC. Sorafenib was shown to directly act on HSCs in rats and attenuate liver fibrosis by reducing HSC proliferation

[31]. Sorafenib might exert its therapeutic effect by suppressing senescent HSCs with enhanced ERK1/2 activation, leading to the alleviation of HCC.

Boosting specific immune cell populations may be effective in controlling senescent HSCs, because natural killer cells have been suggested to selectively kill senescent HSCs [11]. However, many issues remain to be solved to understand the importance of senescent HSCs in human liver disease including HCC; 1) A specific marker of senescent HSCs is currently lacking; 2) Qualitative and quantitative information on senescence-associated secretory factors have been limited in patients. Future studies are vitally required to establish a concept of the manipulation of senescent HSCs to cure liver cancers.

In conclusion, we identified senescence-associated secretory factors regulated by ERK1/2 pathways that were also activated in senescent hHSCs and hDFs. These results revealed a novel role of ERK1/2 in hHSCs, suggesting that the simultaneous induction of *ANGPTL4*, *IL-8*, and *PF4V1* gene can serve as a cell senescence marker in hHSCs. This study may provide a clue about the pathophysiological roles of senescent HSCs in HCC and the possibility of therapeutic targeting of senescent HSCs.

Acknowledgments

We thank Atsuko Daikoku (Osaka City University), Kenji Kitamura (Osaka City University) and Junko Kawawaki (Research support platform of Osaka City University Graduate School of Medicine) for technical assistance.

Grants

This work was supported by The Uehara Memorial Foundation, The Osaka Medical Research Foundation for Intractable Diseases, The Tokyo Biochemical Research Foundation, The Osaka City University Strategic Research Grant 2016 for young researchers, JSPS KAKENHI Grant Number JP26870501 and JP17K18012, and a Grant for Research Program on Hepatitis from the Japan Agency for Medical Research and Development (AMED) Grant Number 16fk0210104h0001.

Disclosures

No conflicts of interest, financial or otherwise, are declared by the authors

Author contributions

N.O. and T.M. designed the experiments and interpreted the results. N.O., T.M., M.H., S.T., H.U., M.S.M., and Y. T. conducted the experiments and prepared the figures. N.O., T.M., K.Y., N.K., and K.I. wrote and revised the manuscript.

Figure legends

Figure 1. Generation of senescent HSCs by replicative passaging.

(A) Calculated doubling time of HHSteCs at passages 5, 17, and 27. (B) Expression of senescence-associated β-galactosidase (SA-βGal). Normal cells (NCs) and senescent cells (SCs) represent HHSteCs at passages 10 and 31, respectively. These cells were stained using the SA-βGal staining kit (left). Bold bars represent 200 μm. SA-βGal-positive cells were counted and the value was calculated as the percentage ratio of SA-βGal-positive cells to the total cells. The data are expressed as means of four individual fields (centre). qPCR analysis of galactosidase beta 1 (GLB1) mRNA (right). The data are expressed as means and SD (n = 3). (C) Western blot analysis of phosphorylated H2A histone family member X (γH2AX) and $p21^{Waf1/Cip1}$ proteins. Total H2AX and glyceraldehyde-3-phosphate dehydrogenase (GAPDH) were used as loading controls, respectively. (D) Flow cytometry analysis of the DNA amounts using Vybrant® DyeCycle™ Green. The percentage ratios of diploid (2N) and tetraploid (4N) cells to total cells are indicated in the figure. (E) Immunofluorescence staining analysis of CDT1 proteins (red). 4',6-Diamidino-2-phenylindole (DAPI) was used for nuclear counterstaining. The yellow bars represent 100 μm in the photos. (F) qPCR analysis of the mRNA expressions of HSCs-related genes (left) and senescence-associated secretory phenotype-related genes (right). The data are expressed as means and SD (n=3-4). Significance was determined by unpaired t test (*, $P<0.05$). (G) IL-8 protein

concentrations in culture medium. The data are expressed as means and SD (n=3). Significance was determined by unpaired t test (*, P<0.05).

Figure 2. Gene expression analysis of secretory genes in SCs.

(A) Microarray gene expression analysis. Twenty-five genes encoding secretory proteins were identified as up-regulated genes in SCs (4.5-fold increase). (B and C) qPCR analysis of the secretory gene expressions in the SCs of Lot 1 and Lot 2. The column and bar represent mean and SD, respectively (n=3-5). Significant increased values greater than 2-fold are summarized in the C panel. Significance was determined by unpaired Student t-test (P<0.05).

Figure 3. ERK1/2 signalling is involved in the regulation of senescence-associated secretory factors in HSCs. (A) Western blot analysis of major mitogen-activated protein kinase pathways in the SCs of HHSteC. (B) Western blot analysis of ERK1/2 and MEK1/2 phosphorylations. ERK1/2 phosphorylation levels were quantified. The signal intensity was measured using image J. The signal intensity of the phosphorylated protein was normalized to that of total protein. The data are expressed as a ratio to means of NCs. Significance was determined by unpaired Student t-test (p<0.05). (C) Western blot analysis of phosphorylated ERK1/2 in nuclear proteins of NCs and SCs (0.3 μg). Cytosolic proteins of SCs (1.5 μg) was used to investigate contamination of

cytosolic proteins in nuclear fraction. Lamin B1 (LMNB1) and GAPDH were used as loading control of nuclear and cytosol fractions, respectively. (D) Effect of treatment with SCH772984 on the expression of senescence-associated secretory genes in SCs. The column and bar represent mean and SD, respectively (n=3). Significance was determined by one-way ANOVA with Dunnett's test (*, $P<0.05$). (E) Change in the phosphorylated ERK1/2 levels of HHSteCs after replicative passaging. 5, 17 and 27 indicate the passage number. (F) Western blot analysis of ERK1/2 phosphorylation after treatment with human EGF. (G) qPCR analysis of ANGPTL4, CCL7, IL-8, PF4V1 and TNFSF15 mRNAs after EGF treatment. The column and bar represent mean and SD, respectively (n=3). Significance was determined by one-way ANOVA with Dunnett's test (*, $P<0.05$).

Figure.4. Enhancement of ERK1/2 phosphorylation and induction of ERK-related gene expression were observed in the senescent human DFs (hDFs).

(A) Expression of SA-βGal in hDFs at passage 7 (NC) and 26 (SC). These cells were stained using the SA-βGal staining kit (left). Bold bars represent 200 μm. SA-βGal-positive cells were counted and the value were calculated as percentage ratios of SA-βGal-positive cells to total cells. The data are expressed as means from four individual fields (centre). qPCR analysis of GLB1 mRNA (right). The data are expressed as means and SD (n=3). (B) Western blot analysis of

p21$^{Waf1/Cip1}$ and ERK1/2 phosphorylation in senescent hDFs. GAPDH was used as a loading control. (C) Immunofluorescence staining analysis of p21$^{Waf1/Cip1}$ proteins (green). DAPI was used for nuclear counterstaining. The yellow bars represent 50 μm in the photos. (D) qPCR analysis of secretory factor mRNAs enhanced in senescent HSCs. The column and bar represent mean and SD, respectively (n=3). Significance was determined by unpaired Student t-test (*, $P<0.05$). (E) IL-8 protein concentrations in the culture medium. The column and bar represent mean and SD, respectively (n=3). Significance was determined by unpaired Student t-test (*, $P<0.05$).

Figure 5. Enhancement of ERK1/2 phosphorylation and induction of ANGPTL4, IL-8, and PF4V1 gene expression are observed in X-ray-induced senescent HSCs.

(A) Expression of SA-βGal after exposure to X ray-irradiation. X-SC and X-NC were donated as the X-ray-exposure group and control group, respectively. These cells were stained using the SA-βGal staining kit (left). Bold bars represent 200 μm. SA-βGal-positive cells were counted and the values were calculated as percentage ratios of SA-βGal-positive cells to total cells. The data are expressed as means from four individual fields (centre). qPCR analysis of GLB1 mRNA (right). The data are expressed as means and SD (n=3). (B) Western blot analysis of ERK1/2 phosphorylation and p21$^{Waf1/Cip1}$ in the X-SC group. (C) Sequential analysis of ERK1/2 phosphorylation and p21$^{Waf1/Cip1}$ expression in HHSteCs after X-ray irradiation. GAPDH was used

as a loading control in western blot analysis. (D) qPCR analysis of ERK1/2-related genes revealed in senescent HSCs. Two individual lots of HHSteCs (Lot 1 and Lot 2) were used for analysis. The column and bar represent mean and SD, respectively (n=3). Significance was determined by unpaired Student's t-test (*, $P<0.05$). (E) IL-8 protein concentrations in the culture medium. The column represents average of triplicate values in one experiment.

References

1. Hayflick L, Moorhead PS (1961) The serial cultivation of human diploid cell strains. Exp Cell Res 25:585-621

2. Campisi J, d'Adda di Fagagna F (2007) Cellular senescence: when bad things happen to good cells. Nat Rev Mol Cell Biol 8 (9):729-740. doi:10.1038/nrm2233

3. Serrano M, Lin AW, McCurrach ME, Beach D, Lowe SW (1997) Oncogenic ras provokes premature cell senescence associated with accumulation of p53 and p16INK4a. Cell 88 (5):593-602

4. Collado M, Blasco MA, Serrano M (2007) Cellular senescence in cancer and aging. Cell 130 (2):223-233. doi:10.1016/j.cell.2007.07.003

5. Parrinello S, Coppe JP, Krtolica A, Campisi J (2005) Stromal-epithelial interactions in aging and cancer: senescent fibroblasts alter epithelial cell differentiation. J Cell Sci 118 (Pt 3):485-496. doi:10.1242/jcs.01635

6. Krtolica A, Parrinello S, Lockett S, Desprez PY, Campisi J (2001) Senescent fibroblasts promote epithelial cell growth and tumorigenesis: a link between cancer and aging. Proc Natl Acad Sci U S A 98 (21):12072-12077. doi:10.1073/pnas.211053698

7. Liu D, Hornsby PJ (2007) Senescent human fibroblasts increase the early growth of xenograft tumors via matrix metalloproteinase secretion. Cancer Res 67 (7):3117-3126. doi:10.1158/0008-5472.CAN-06-3452

8. Coppe JP, Boysen M, Sun CH, Wong BJ, Kang MK, Park NH, Desprez PY, Campisi J, Krtolica A (2008) A role for fibroblasts in mediating the effects of tobacco-induced epithelial cell growth and invasion. Mol Cancer Res 6 (7):1085-1098. doi:10.1158/1541-7786.MCR-08-0062

9. Bavik C, Coleman I, Dean JP, Knudsen B, Plymate S, Nelson PS (2006) The gene expression program of prostate fibroblast senescence modulates neoplastic epithelial cell proliferation through paracrine mechanisms. Cancer Res 66 (2):794-802. doi:10.1158/0008-5472.CAN-05-1716

10. Tsuchida T, Friedman SL (2017) Mechanisms of hepatic stellate cell activation. Nat Rev Gastroenterol Hepatol 14 (7):397-411. doi:10.1038/nrgastro.2017.38

11. Krizhanovsky V, Yon M, Dickins RA, Hearn S, Simon J, Miething C, Yee H, Zender L, Lowe SW (2008) Senescence of activated stellate cells limits liver fibrosis. Cell 134 (4):657-667. doi:10.1016/j.cell.2008.06.049

12. Lujambio A, Akkari L, Simon J, Grace D, Tschaharganeh DF, Bolden JE, Zhao Z, Thapar V, Joyce JA, Krizhanovsky V, Lowe SW (2013) Non-cell-autonomous tumor suppression by p53. Cell 153 (2):449-460. doi:10.1016/j.cell.2013.03.020

13. Yoshimoto S, Loo TM, Atarashi K, Kanda H, Sato S, Oyadomari S, Iwakura Y, Oshima K, Morita H, Hattori M, Honda K, Ishikawa Y, Hara E, Ohtani N (2013) Obesity-induced gut microbial metabolite promotes liver cancer through senescence secretome. Nature 499 (7456):97-101. doi:10.1038/nature12347

14. Saito N, Adachi H, Tanaka H, Nakata S, Kawada N, Oofusa K, Yoshizato K (2017) Interstitial fluid flow-induced growth potential and hyaluronan synthesis of fibroblasts in a fibroblast-populated stretched collagen gel culture. Biochim Biophys Acta 1861 (9):2261-2273. doi:10.1016/j.bbagen.2017.06.019

15. Lee BY, Han JA, Im JS, Morrone A, Johung K, Goodwin EC, Kleijer WJ, DiMaio D, Hwang ES (2006) Senescence-associated beta-galactosidase is lysosomal beta-galactosidase. Aging Cell 5 (2):187-195. doi:10.1111/j.1474-9726.2006.00199.x

16. Johmura Y, Shimada M, Misaki T, Naiki-Ito A, Miyoshi H, Motoyama N, Ohtani N, Hara E, Nakamura M, Morita A, Takahashi S, Nakanishi M (2014) Necessary and sufficient role for a mitosis skip in senescence induction. Mol Cell 55 (1):73-84. doi:10.1016/j.molcel.2014.05.003

17. Ebert R, Benisch P, Krug M, Zeck S, Meissner-Weigl J, Steinert A, Rauner M, Hofbauer L, Jakob F (2015) Acute phase serum amyloid A induces proinflammatory cytokines and mineralization via toll-like receptor 4 in mesenchymal stem cells. Stem Cell Res 15 (1):231-239. doi:10.1016/j.scr.2015.06.008

18. Freund A, Laberge RM, Demaria M, Campisi J (2012) Lamin B1 loss is a senescence-associated biomarker. Mol Biol Cell 23 (11):2066-2075. doi:10.1091/mbc.E11-10-0884

19. Shimi T, Butin-Israeli V, Adam SA, Hamanaka RB, Goldman AE, Lucas CA, Shumaker DK, Kosak ST, Chandel NS, Goldman RD (2011) The role of nuclear lamin B1 in cell proliferation and senescence. Genes Dev 25 (24):2579-2593. doi:10.1101/gad.179515.111

20. Kim HS, Song MC, Kwak IH, Park TJ, Lim IK (2003) Constitutive induction of p-Erk1/2 accompanied by reduced activities of protein phosphatases 1 and 2A and MKP3 due to reactive oxygen species during cellular senescence. J Biol Chem 278 (39):37497-37510. doi:10.1074/jbc.M211739200

21. Chien Y, Scuoppo C, Wang X, Fang X, Balgley B, Bolden JE, Premsrirut P, Luo W, Chicas A, Lee CS, Kogan SC, Lowe SW (2011) Control of the senescence-associated secretory phenotype by NF-kappaB promotes senescence and enhances chemosensitivity. Genes Dev 25 (20):2125-2136. doi:10.1101/gad.17276711

22. Kuilman T, Michaloglou C, Vredeveld LC, Douma S, van Doorn R, Desmet CJ, Aarden LA, Mooi WJ, Peeper DS (2008) Oncogene-induced senescence relayed by an interleukin-dependent inflammatory network. Cell 133 (6):1019-1031. doi:10.1016/j.cell.2008.03.039

23. Freund A, Patil CK, Campisi J (2011) p38MAPK is a novel DNA damage response-

independent regulator of the senescence-associated secretory phenotype. EMBO J 30 (8):1536-1548. doi:10.1038/emboj.2011.69

24. Herranz N, Gallage S, Mellone M, Wuestefeld T, Klotz S, Hanley CJ, Raguz S, Acosta JC, Innes AJ, Banito A, Georgilis A, Montoya A, Wolter K, Dharmalingam G, Faull P, Carroll T, Martinez-Barbera JP, Cutillas P, Reisinger F, Heikenwalder M, Miller RA, Withers D, Zender L, Thomas GJ, Gil J (2015) mTOR regulates MAPKAPK2 translation to control the senescence-associated secretory phenotype. Nat Cell Biol 17 (9):1205-1217. doi:10.1038/ncb3225

25. Laberge RM, Sun Y, Orjalo AV, Patil CK, Freund A, Zhou L, Curran SC, Davalos AR, Wilson-Edell KA, Liu S, Limbad C, Demaria M, Li P, Hubbard GB, Ikeno Y, Javors M, Desprez PY, Benz CC, Kapahi P, Nelson PS, Campisi J (2015) MTOR regulates the pro-tumorigenic senescence-associated secretory phenotype by promoting IL1A translation. Nat Cell Biol 17 (8):1049-1061. doi:10.1038/ncb3195

26. Nakayama T, Hirakawa H, Shibata K, Nazneen A, Abe K, Nagayasu T, Taguchi T (2011) Expression of angiopoietin-like 4 (ANGPTL4) in human colorectal cancer: ANGPTL4 promotes venous invasion and distant metastasis. Oncol Rep 25 (4):929-935. doi:10.3892/or.2011.1176

27. Lee YS, Choi I, Ning Y, Kim NY, Khatchadourian V, Yang D, Chung HK, Choi D, LaBonte MJ, Ladner RD, Nagulapalli Venkata KC, Rosenberg DO, Petasis NA, Lenz HJ, Hong YK (2012) Interleukin-8 and its receptor CXCR2 in the tumour microenvironment promote colon cancer growth, progression and metastasis. Br J Cancer 106 (11):1833-1841. doi:10.1038/bjc.2012.177

28. Quemener C, Baud J, Boye K, Dubrac A, Billottet C, Soulet F, Darlot F, Dumartin L, Sire M, Grepin R, Daubon T, Rayne F, Wodrich H, Couvelard A, Pineau R, Schilling M, Castronovo V, Sue SC, Clarke K, Lomri A, Khatib AM, Hagedorn M, Prats H, Bikfalvi A (2016) Dual Roles for CXCL4 Chemokines and CXCR3 in Angiogenesis and Invasion of Pancreatic Cancer. Cancer Res 76 (22):6507-6519. doi:10.1158/0008-5472.CAN-15-2864

29. Zhu B, Lin N, Zhang M, Zhu Y, Cheng H, Chen S, Ling Y, Pan W, Xu R (2015) Activated hepatic stellate cells promote angiogenesis via interleukin-8 in hepatocellular carcinoma. J Transl Med 13:365. doi:10.1186/s12967-015-0730-7

30. Li H, Ge C, Zhao F, Yan M, Hu C, Jia D, Tian H, Zhu M, Chen T, Jiang G, Xie H, Cui Y, Gu J, Tu H, He X, Yao M, Liu Y, Li J (2011) Hypoxia-inducible factor 1 alpha-activated angiopoietin-like protein 4 contributes to tumor metastasis via vascular cell adhesion molecule-1/integrin beta1 signaling in human hepatocellular carcinoma. Hepatology 54 (3):910-919. doi:10.1002/hep.24479

31. Wang Y, Gao J, Zhang D, Zhang J, Ma J, Jiang H (2010) New insights into the antifibrotic

effects of sorafenib on hepatic stellate cells and liver fibrosis. J Hepatol 53 (1):132-144. doi:10.1016/j.jhep.2010.02.027

Figure 1

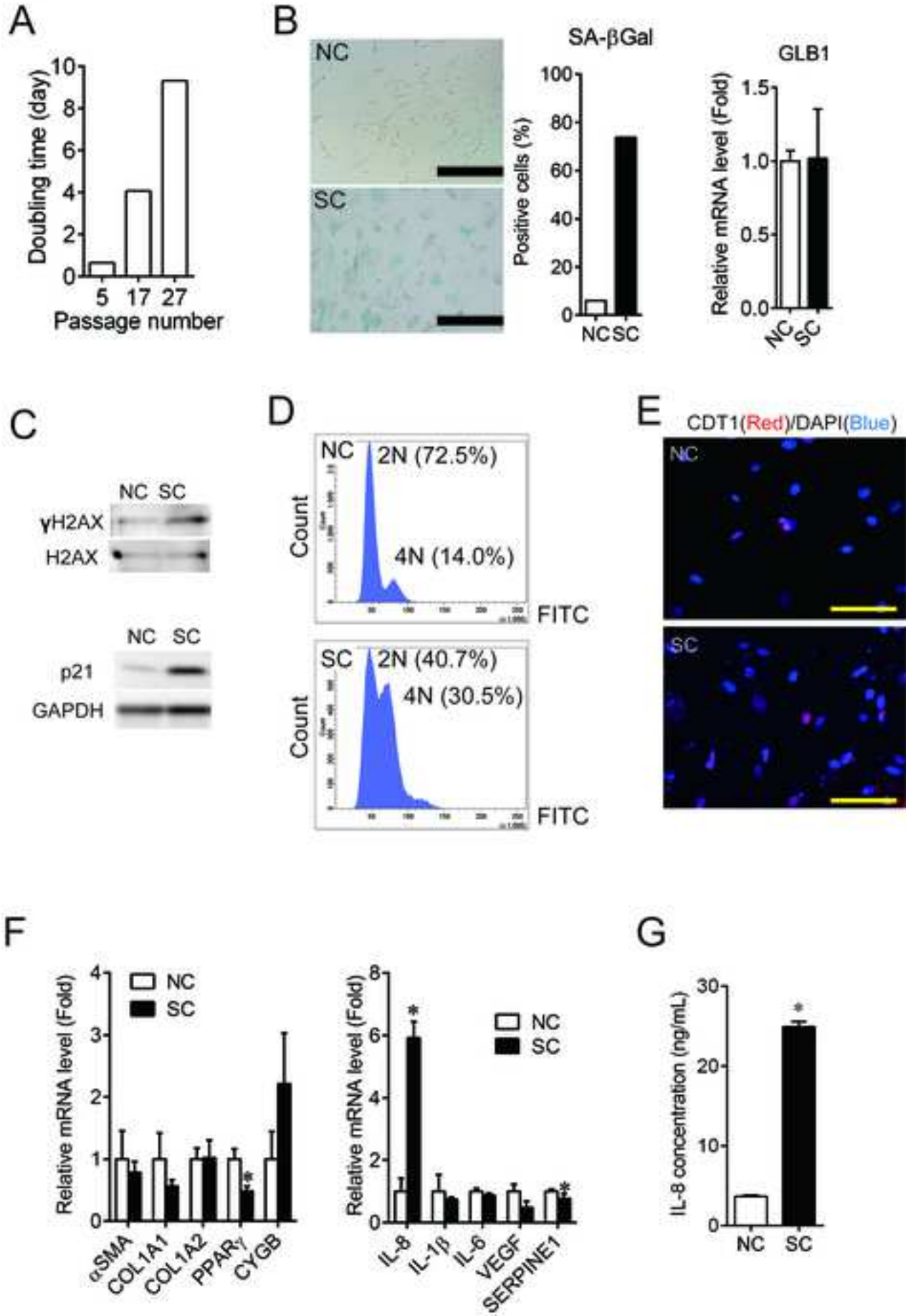
A
Doubling time (day)
10
8
6
4
2
0
5 17 27
Passage number
B
NC
SC
SA-βGal
Positive cells (%)
100
80
60
40
20
0
NC SC
GLB1
Relative mRNA level (Fold)
1.5
1.0
0.5
0.0
NC SC
C
NC SC
γH2AX
H2AX
NC SC
p21
GAPDH
D
NC
2N (72.5%)
4N (14.0%)
Count
FITC
SC
2N (40.7%)
4N (30.5%)
Count
FITC
E
CDT1(Red)/DAPI(Blue)
NC
SC
F
Relative mRNA level (Fold)
NC
SC
αSMA
COL1A1
COL1A2
PPARγ
CYGB
Relative mRNA level (Fold)
NC
SC
IL-8
IL-1β
IL-6
VEGF
SERPINE1
G
IL-8 concentration (ng/mL)
30
20
10
0
NC SC

Figure 2

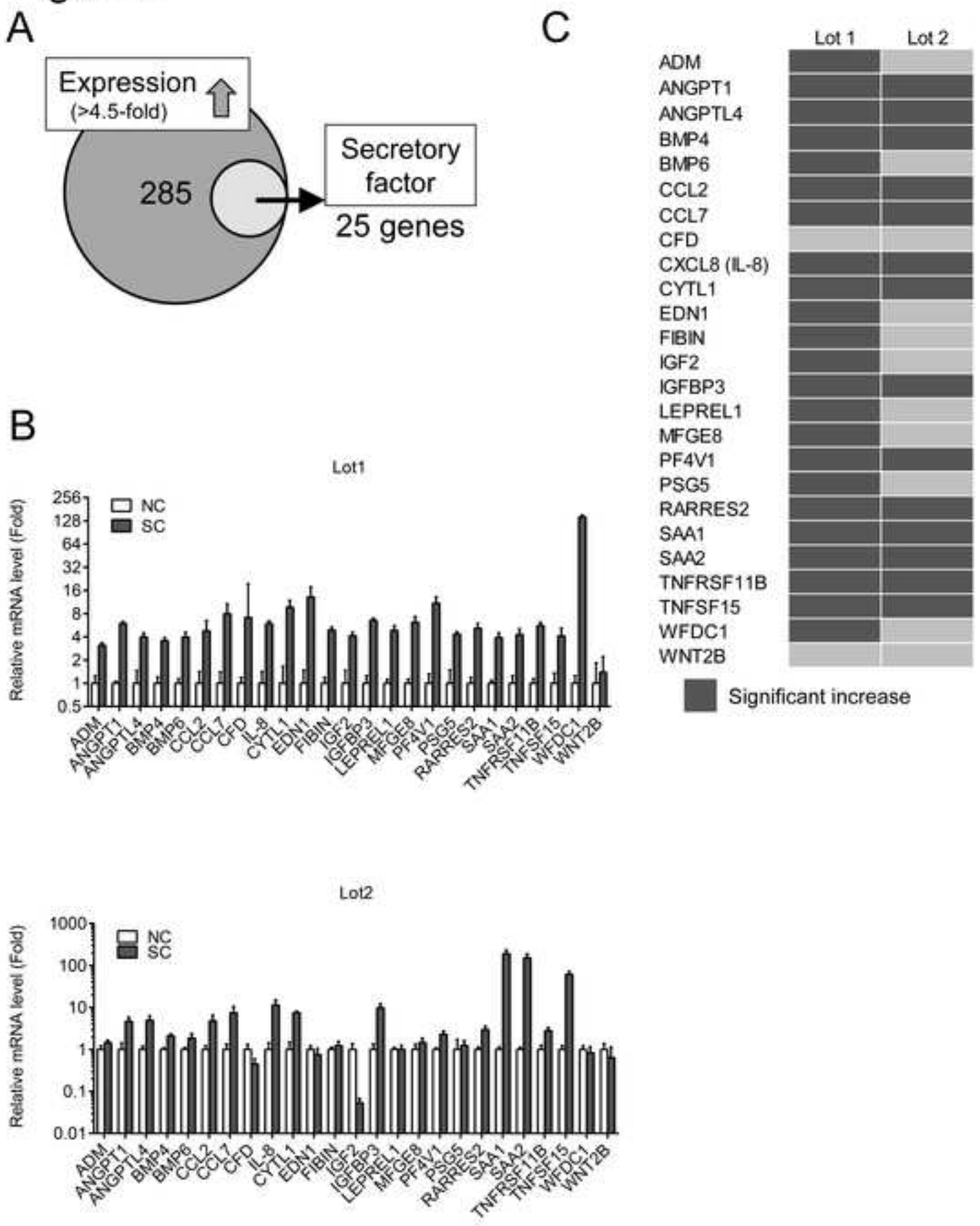
Figure 2
A
Expression
(>4.5-fold)
285
Secretory
factor
25 genes
B
Lot1
Relative mRNA level (Fold)
NC
SC
256
128
64
32
16
8
4
2
1
0.5
ADM
ANGPT1
ANGPTL4
BMP4
BMP6
CCL2
CCL7
CFD
IL-8
CYTL1
EDN1
FIBIN
IGF2
IGFBP3
LEPREL1
MFGE8
PF4V1
PSG5
RARRES2
SAA1
SAA2
TNFRSF11B
TNFSF15
WFDC1
WNT2B
Lot2
Relative mRNA level (Fold)
NC
SC
1000
100
10
1
0.1
0.01
ADM
ANGPT1
ANGPTL4
BMP4
BMP6
CCL2
CCL7
CFD
IL-8
CYTL1
EDN1
FIBIN
IGF2
IGFBP3
LEPREL1
MFGE8
PF4V1
PSG5
RARRES2
SAA1
SAA2
TNFRSF11B
TNFSF15
WFDC1
WNT2B
C
Lot 1
Lot 2
ADM
ANGPT1
ANGPTL4
BMP4
BMP6
CCL2
CCL7
CFD
CXCL8 (IL-8)
CYTL1
EDN1
FIBIN
IGF2
IGFBP3
LEPREL1
MFGE8
PF4V1
PSG5
RARRES2
SAA1
SAA2
TNFRSF11B
TNFSF15
WFDC1
WNT2B
Significant increase

Figure 3

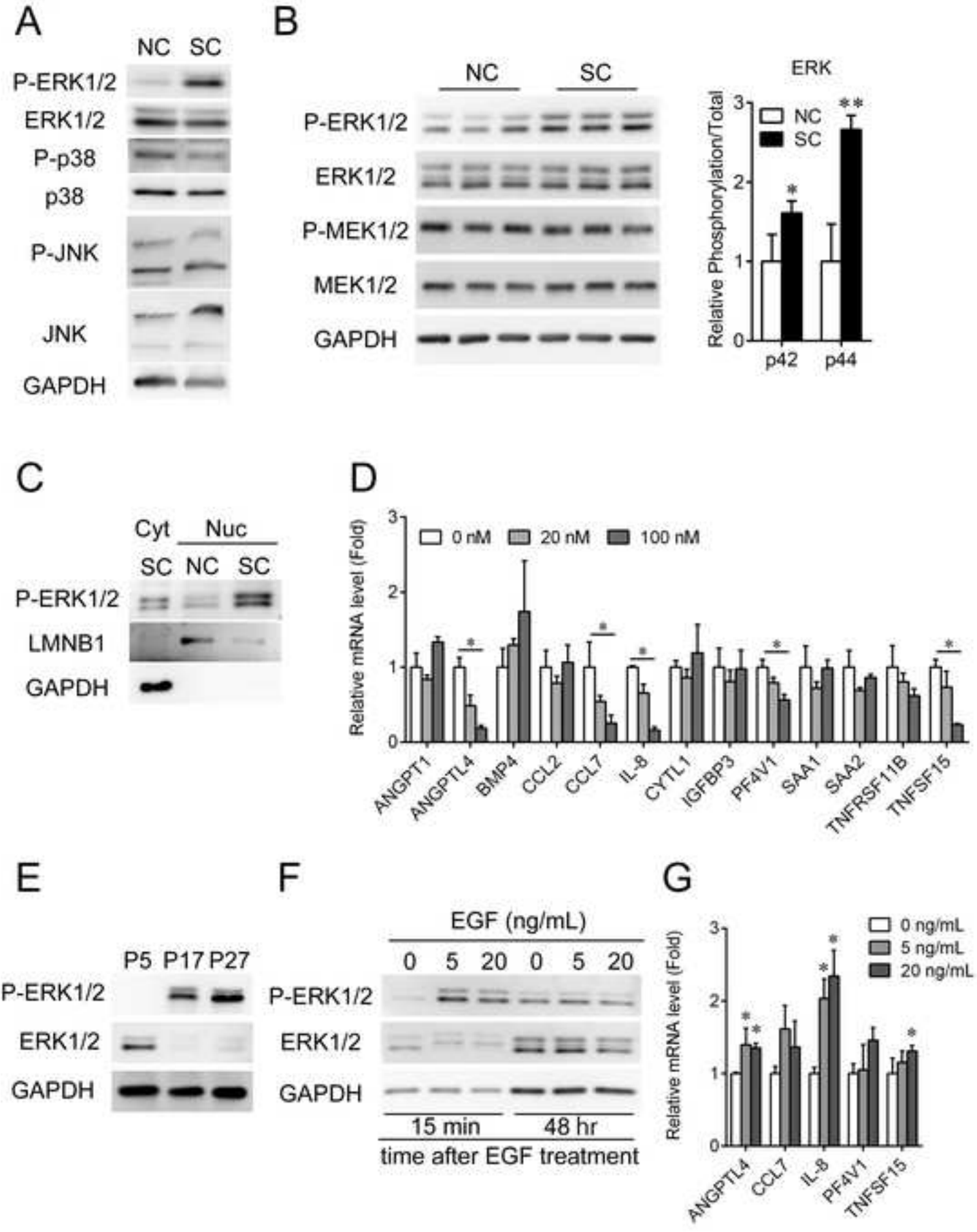
A
NC
SC
P-ERK1/2
ERK1/2
P-p38
p38
P-JNK
JNK
GAPDH
B
NC
SC
P-ERK1/2
ERK1/2
P-MEK1/2
MEK1/2
GAPDH
ERK
NC
SC
Relative Phosphorylation/Total
p42
p44
C
Cyt
Nuc
SC
NC
SC
P-ERK1/2
LMNB1
GAPDH
D
0 nM
20 nM
100 nM
Relative mRNA level (Fold)
ANGPT1
ANGPTL4
BMP4
CCL2
CCL7
IL-8
CYTL1
IGFBP3
PF4V1
SAA1
SAA2
TNFRSF11B
TNFSF15
E
P5
P17
P27
P-ERK1/2
ERK1/2
GAPDH
F
EGF (ng/mL)
0
5
20
0
5
20
P-ERK1/2
ERK1/2
GAPDH
15 min
48 hr
time after EGF treatment
G
0 ng/mL
5 ng/mL
20 ng/mL
Relative mRNA level (Fold)
ANGPTL4
CCL7
IL-8
PF4V1
TNFSF15

Figure 4

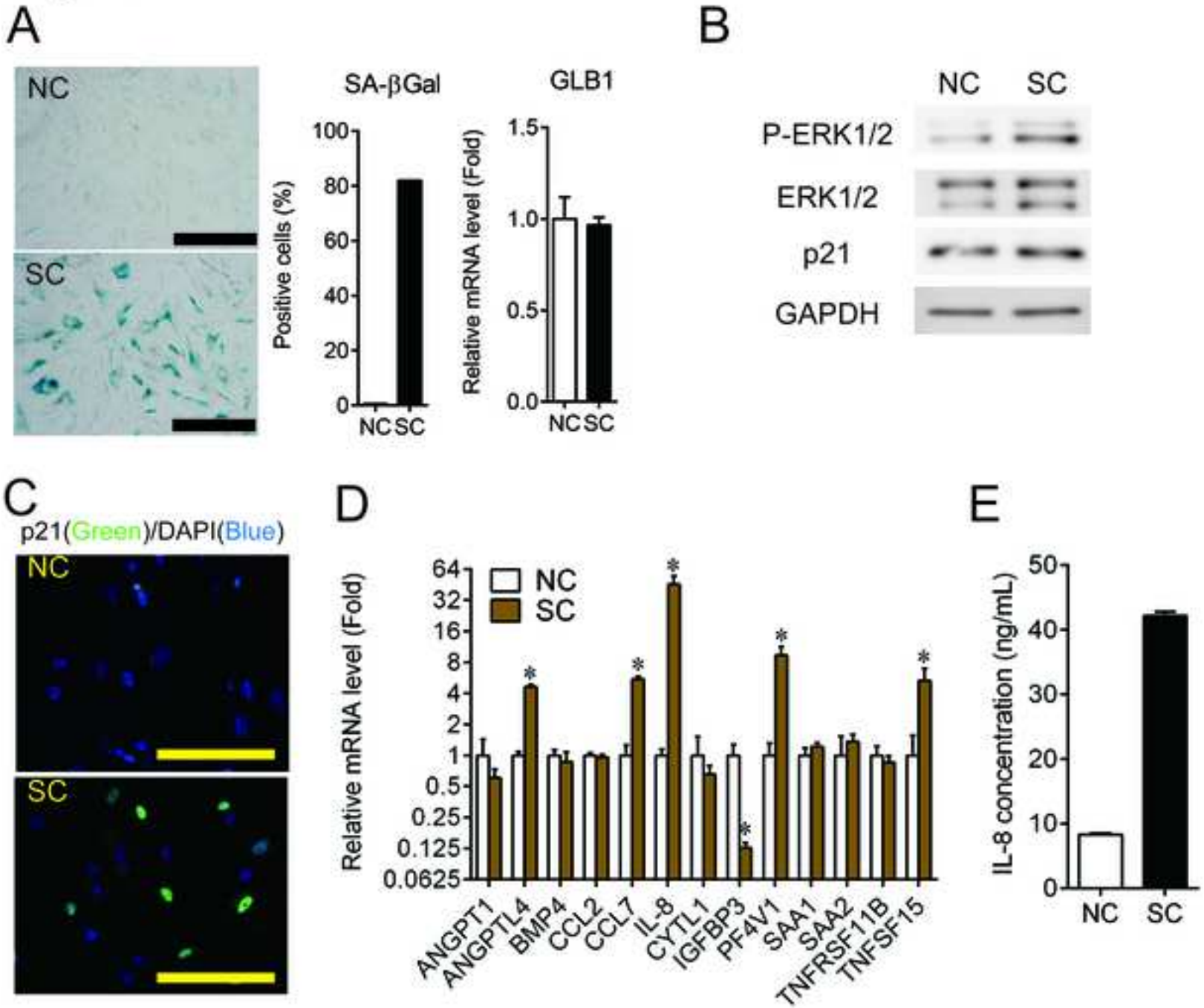
A
NC
SC
SA-βGal
Positive cells (%)
100
80
60
40
20
0
NC SC
GLB1
Relative mRNA level (Fold)
1.5
1.0
0.5
0.0
NC SC
B
NC SC
P-ERK1/2
ERK1/2
p21
GAPDH
C
p21(Green)/DAPI(Blue)
NC
SC
D
Relative mRNA level (Fold)
64
32
16
8
4
2
1
0.5
0.25
0.125
0.0625
NC
SC
ANGPT1
ANGPTL4
BMP4
CCL2
CCL7
IL-8
CYTL1
IGFBP3
PF4V1
SAA1
SAA2
TNFRSF11B
TNFSF15
E
IL-8 concentration (ng/mL)
50
40
30
20
10
0
NC SC

Figure 5

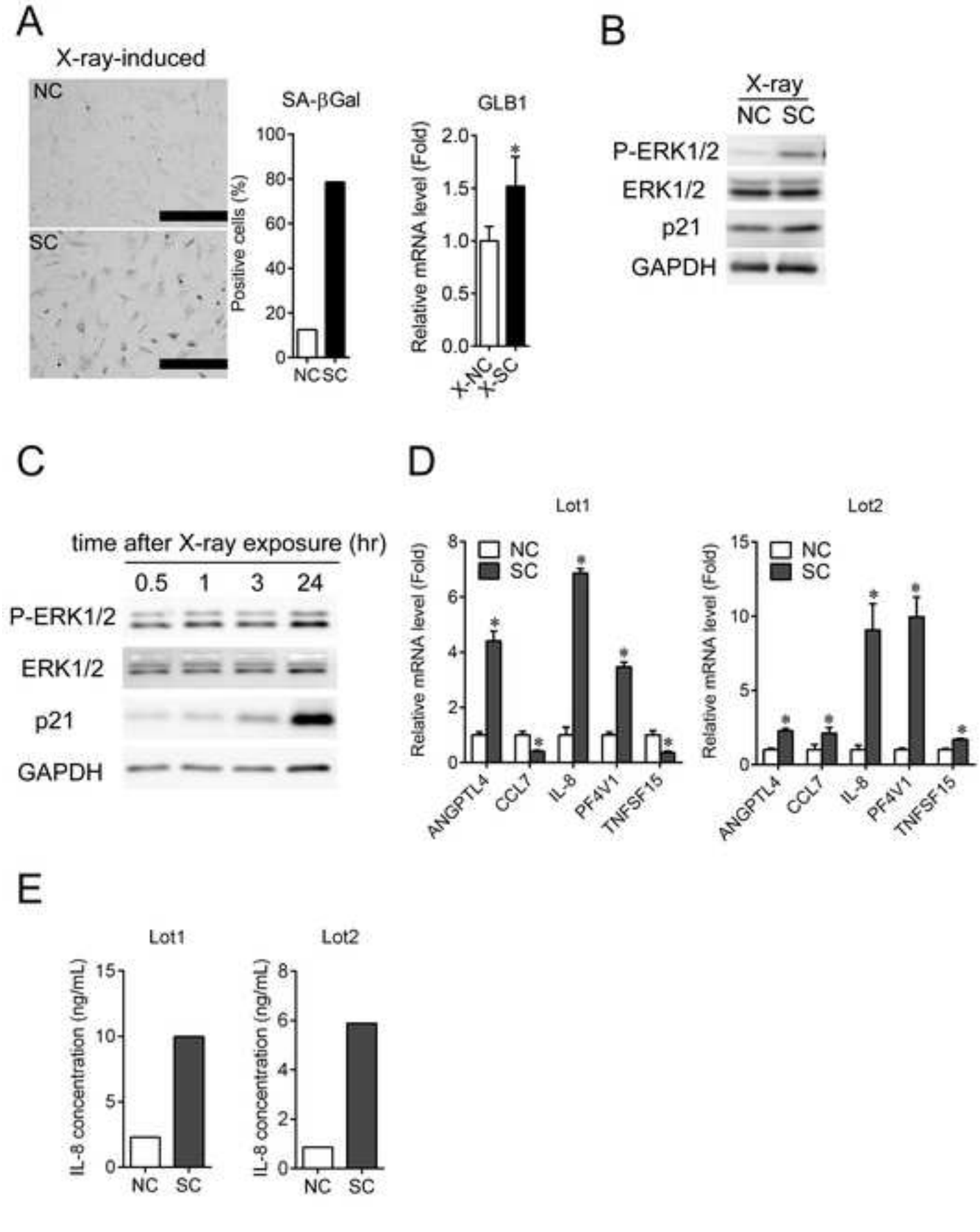
A
X-ray-induced
NC
SC
SA-βGal
Positive cells (%)
100
80
60
40
20
0
NC SC
GLB1
Relative mRNA level (Fold)
2.0
1.5
1.0
0.5
0.0
*
X-NC
X-SC
B
X-ray
NC SC
P-ERK1/2
ERK1/2
p21
GAPDH
C
time after X-ray exposure (hr)
0.5 1 3 24
P-ERK1/2
ERK1/2
p21
GAPDH
D
Lot1
Lot2
Relative mRNA level (Fold)
NC
SC
ANGPTL4
CCL7
IL-8
PF4V1
TNFSF15
E
Lot1
Lot2
IL-8 concentration (ng/mL)
NC SC

Table 1. Primary antibodies used in this study.

Anti-	Company	Cat. No
$p21^{Waf1/Cip1}$	Cell Signaling Technology	#2947
phospho-MEK1/2	Cell Signaling Technology	#9154
MEK1/2	Cell Signaling Technology	#8727
phospho-ERK1/2	Cell Signaling Technology	#4370
ERK1/2	Cell Signaling Technology	#4695
phospho-p38	Cell Signaling Technology	#4511
p38	Cell Signaling Technology	#8690
phospho-SAPK/JNK	Cell Signaling Technology	#4668
SAPK/JNK	Cell Signaling Technology	#9252
phospho-histone H2AX (γH2AX)	Cell Signaling Technology	#2577
histone H2AX	Cell Signaling Technology	#7631
CDT1	Abcam	Ab202067
LMNB1	Santa Cruz Biotechnology	SC374015
GAPDH	Millipore	MAB374

Table 2. Primers used in this study.

Gene	Forward (5' to 3')	Reverse (5' to 3')
18S	CAGCCACCCGAGATTGAGCA	TAGTAGCGACGGGCGGTGTG
GLB1	CTCCTTCTGCTGCTGGTTC	GGAGTCCCGGCTATAGTCAA
αSMA	CAGCCAAGCACTGTCAGG	CCAGAGCCATTGTCACACAC
COL1A1	AAGAGGAAGGCCAAGTCGAG	CACACGTCTCGGTCATGGTA
COL1A2	GAAAAGGAGTTGGACTTGGC	AGCAGGTCCTTGGAAACCTT
PPARγ	AGGCCATTTTCTCAAACGAG	GAGAGATCCACGGAGCTGAT
CYGB	CGAGATGGAGATCGAGCG	CGAGGGGAAGTTCACAAAGA
IL-8	CAAGAGCCAGGAAGAAACCA	AGCACTCCTTGGCAAAACTG
IL-1β	GAAGCTGATGGCCCTAAACA	AAGCCCTTGCTGTAGTGGTG
IL-6	AGTGAGGAACAAGCCAGAGC	CATTTGTGGTTGGGTCAGG
SERPINE1	AGAAACCCAGCAGCAGATTC	TGGTGCTGATCTCATCCTTG
VEGF	CTACCTCCACCATGCCAAGT	AGCTGCGCTGATAGACATCC
WFDC1	CTACGCCTGCCTAGAAGCTG	ACGCCTCTGCTTGTAACACC
CYTL1	TTCAACCTCCTGCAGGTCTC	GGAATCTACCTGGGCCACTT
EDN1	CAAGGAGCTCCAGAAACAGC	TTTATCCATCAGGGACGAGC
PF4V1	GAGATGCTGTTCTTGGCGTT	GGAGGTGGTCTTCACACACA
IGFBP3	AACGCTAGTGCCGTCAGC	GACGGGCTCTCCACACTG
MFGE8	AGATTGTACCCCACGAGCTG	GCTGTTATTCTTCAGGCCCA
CFD	TTGATGTGCGCGGAGAG	GAGGTGACCACGCCCTC
CCL7	CTGCTTTCAGCCCCCAG	AGCTCTCCAGCCTCTGCTTA
CCL2	GCCTCCAGCATGAAAGTCTC	AGGTGACTGGGGCATTGAT
PSG5	GGAACCTGCCTATCACTGCT	TGTAATGGTAGAGGTCCATCAG
LEPREL1	CGCAGAGTGCCCTACAACTA	ATGTGCTCAGGGTTAGCCAC
ANGPT1	ACCGGATTTCTCTTCCCAGA	CCGACTTCATGTTTTCCACA
WNT2B	GACGGCAGTACCTGGCATAC	TGTCACAGATCACTCGTGCC
SAA2	TGGTTTTCTGCTCCTTGGTC	GTAGGCTCTCCACATGTCCC
BMP6	CATGAGCTTTGTGAACCTGG	CACCTCACCCTCAGGAATCT
TNFRSF11B	GGGGACCACAATGAACAAGT	GCTGATGAGAGGTTTCTTCG
TNFSF15	CACATACCTGCTTGTCAGCC	TGTGAAGGTGCAAACTCCTG
FIBIN	GGCTCAACGAGGACTTTCTG	GCTCGTATTTGTCCCTGAGC

Table 2. Primers used in this study (Continued).

Gene	Forward (5' to 3')	Reverse (5' to 3')
RARRES2	AGAGGGACTGGAAGAAACCC	TTTGTCCTCAGAGCCCAGTT
IGF2	CTGTTCGGTTTGCGACAC	CCAAGAAGGTGAGAAGCACC
BMP4	TGAGCCTTTCCAGCAAGTTT	GCATTCGGTTACCAGGAATC
ANGPTL4	GAGATGGCCCAGCCAGTT	TAGTCCACTCTGCCTCTCCC
ADM	GCTTGGACTTCGGAGTTTTG	ACGGAAACCAGCTTCATCC
SAA1	AGCCGAAGCTTCTTTTCGTT	GCCGATGTAATTGGCTTCTC

18S, 18 S ribosomal RNA; GLB1, galactosidase beta 1; αSMA, alpha-smooth muscle actin; COL1A1, collagen type I alpha 1; COL1A2, collagen type I alpha 2; PPARγ, peroxisome proliferator-activated receptor gamma; CYGB, cytoglobin; SERPINE1, serpin family E member 1; WFDC1, WAP four-disulfide core domain 1; CYTL1, cytokine like 1; EDN1, endothelin 1; PF4V1, platelet factor 4 variant 1; IGFBP3, insulin like growth factor binding protein 3; MFGE8, milk fat globule-EGF factor 8 protein; CFD, complement factor D; CCL7, C-C motif chemokine ligand 7; CCL2, C-C motif chemokine ligand 2; PSG5, pregnancy specific beta-1-glycoprotein 5; LEPREL1, prolyl 3-hydroxylase 2; ANGPT1, angiopoietin 1; WNT2B, Wnt family member 2B; SAA2, serum amyloid A2; BMP6, bone morphogenetic protein 6; TNFRSF11B, TNF receptor superfamily member 11b; TNFSF15, TNF superfamily member 15; FIBIN, fin bud initiation factor homolog (zebrafish); RARRES2, retinoic acid receptor responder 2; IGF2, insulin like growth factor 2; BMP4, bone morphogenetic protein 4; ANGPTL4, angiopoietin like 4; ADM, adrenomedullin; SAA1, serum amyloid A1.

Table 3. 25 genes selected from microarray analysis.

Gene Symbol	Description	SC/NC
WFDC1	WAP Four-Disulfide Core Domain 1	193.20
CYTL1	Cytokine Like 1	29.94
EDN1	Endothelin 1	12.50
PF4V1	Platelet Factor 4 Variant 1	10.63
IGFBP3	Insulin Like Growth Factor Binding Protein 3	10.28
MFGE8	Milk Fat Globule-EGF Factor 8 Protein	9.57
CFD	Complement Factor D	9.52
CCL7	C-C Motif Chemokine Ligand 7	9.09
CCL2	C-C Motif Chemokine Ligand 2	8.45
CXCL8 (IL-8)	C-X-C Motif Chemokine Ligand 8 (Interleukin-8)	7.31
PSG5	Pregnancy Specific Beta-1-Glycoprotein 5	6.98
LEPREL1	Leprecan-Like Protein 1	6.59
ANGPT1	Angiopoietin 1	6.57
WNT2B	Wnt Family Member 2B	6.27
SAA2	Serum Amyloid A2	6.11
BMP6	Bone Morphogenetic Protein 6	6.06
TNFRSF11B	Tumor Necrosis Factor Receptor Superfamily, Member 11b	6.05
TNFSF15	Tumor Necrosis Factor Superfamily Member 15	5.63
FIBIN	Fin Bud Initiation Factor Homolog (Zebrafish)	5.54
RARRES2	Retinoic Acid Receptor Responder 2	5.17
IGF2	Insulin Like Growth Factor 2	5.04
BMP4	Bone Morphogenetic Protein 4	4.93
ANGPTL4	Angiopoietin Like 4	4.81
ADM	Adrenomedullin	4.80
SAA1	Serum Amyloid A1	4.59